低周波電波とX線で探る銀河団磁場

滝沢元和、高橋律裕、高橋育美（山形大）、
小澤武揚（国立天文台）、赤堀卓也（鹿児島大）、
中西裕之（鹿児島大）、祖父江義明（東大）他

日本SKA合同サイエンス会議「宇宙磁場：銀河系内現象から大規模構造へ」
2016年10月27日(木)-29日(土)＠ルーセントタカミヤ（山形蔵王）

Observational Evidence of Intracluster Magnetic Field (1): Radio Halos / Relics

南の三角座銀河団の電波ハロー (Bernardi et al. 2016)
XMM X-ray image (colors) KAT-7 Radio image (white contours)
二つ後の鷹箸講演で

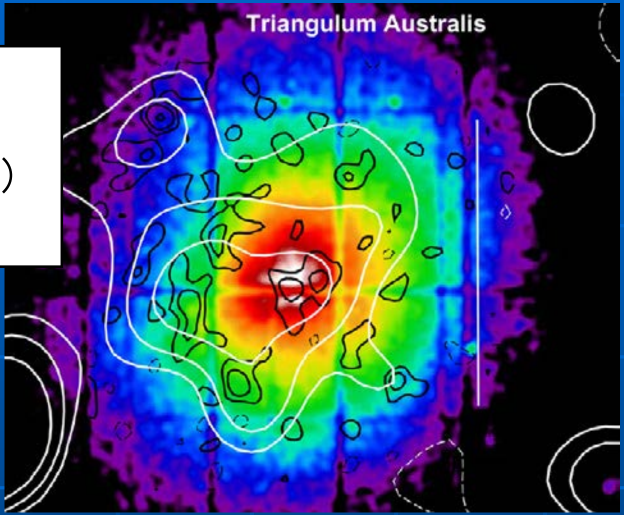

Non-thermal diffuse radio emission from merging clusters of galaxies

synchrotron radio

$\gamma \sim 10^4$ electrons + 0.1-10μG B

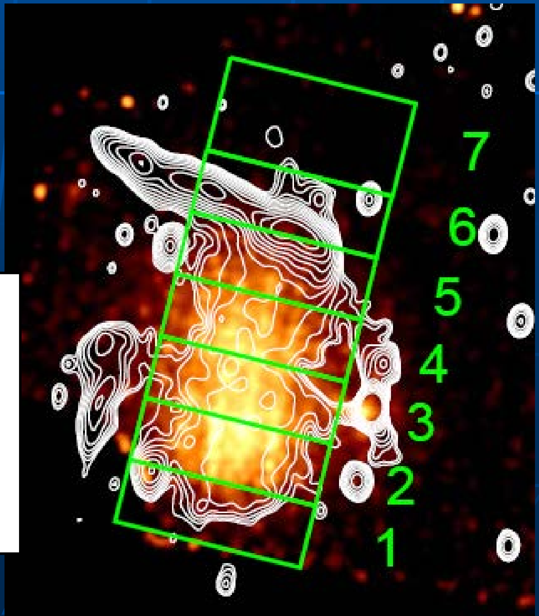

1RXS J0603.3+4214 with "Toothbrush"Radio Relic
Suzaku X-ray image (colors) Radio image (contours)
Itahana et al. (2015)
Relicについてはこの後の板花さんの講演で

Observational Evidence of Intracluster Magnetic Field (2): Faraday Rotation

- Polarized plains of linear polarized radio wave rotate when propagating through the magnetized plasma.

$$\Delta\theta = \frac{2\pi e^3}{m^2 c^2 \omega^2} \int_0^d n B_{\parallel} ds.$$

- Polarized radio sources observations in and behind clusters suggest random magnetic field structures.

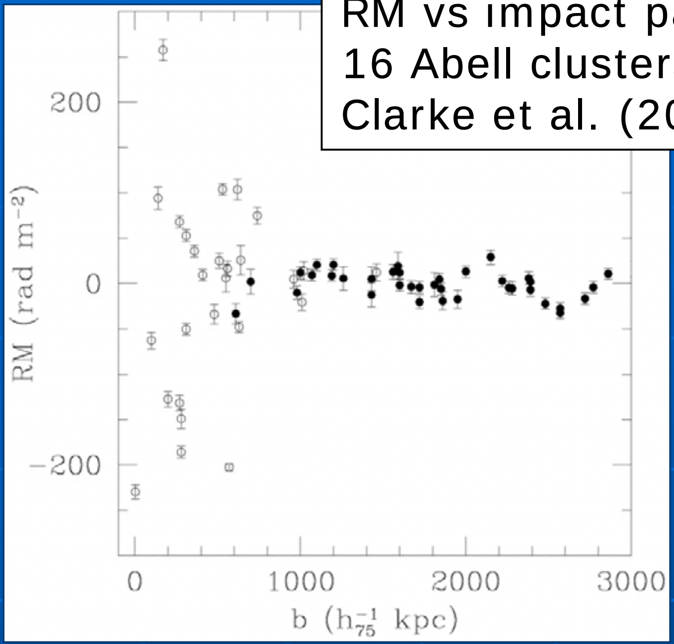

RM vs impact paameter for 16 Abell clusters
Clarke et al. (2001)

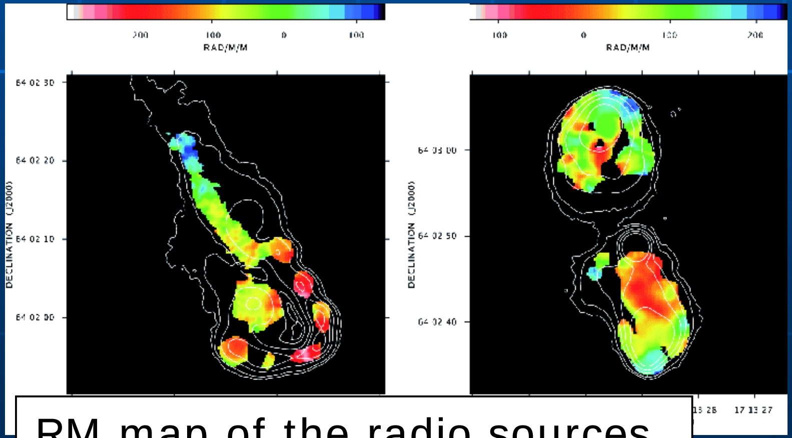

RM map of the radio sources in Abell 2255
Govoni et al. (2006)

Intracluster Magnetic Field

- There is random magnetic field in the intracluster space, whose typical strength is ~ μG.
  - Shyncrotron radio halos/relics
  - Faraday rotation measure
- $P_B \sim 0.01 P_{th}$ not important?
  - suppression of fluid instabilities
  - suppression of heat conduction
  - Particle acceleration (magnetic turbulence, shock)
- Not only field strength, but also field structures are important.

Abell 2199と電波銀河NGC6166

- 典型的な冷却コア銀河団。
- 中心に電波銀河
- 周囲のICMと電波ローブが相互作用

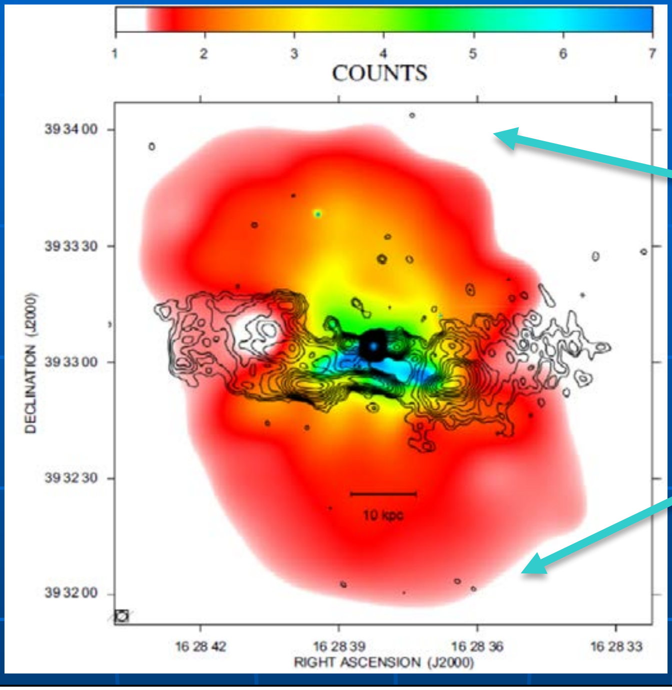

NGC 6166
カラー:X線(Chandra)、コントア:電波
Vacca+ 2012

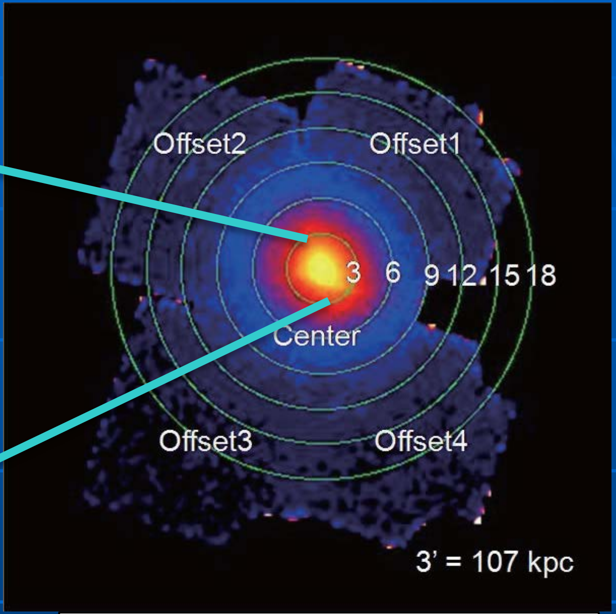

Abell2199
カラー:X線(Suzaku)
Kawaharada+ 2010

JVLAで偏波観測 ⇒ RMから磁場の推定を試みた

A2199中心部：RMマップ と RMヒストグラム

ビームサイズ 5.4”

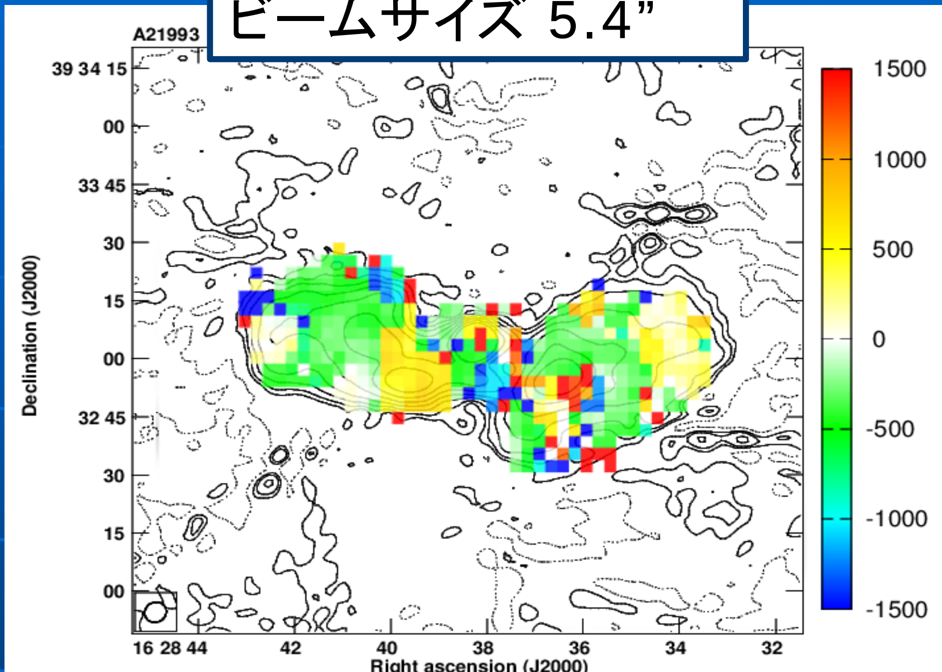

$$\langle\overline{\mathrm{RM}}\rangle \sim -53.65\ [\mathrm{rad/m^2}]$$

$$\sigma_{RM} \sim\ 779.16\ [\mathrm{rad/m^2}]$$

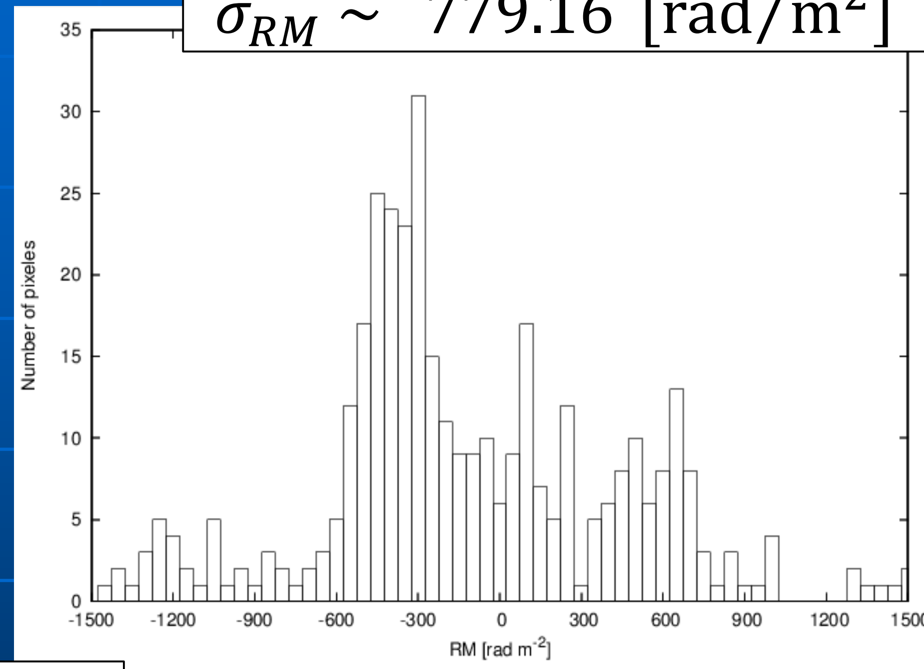

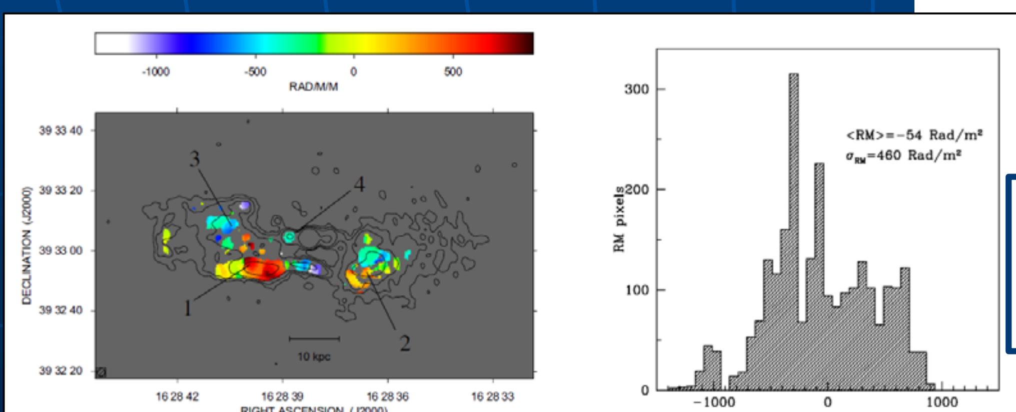

Vacca et al.(2012)と比較するとRMの得られた範囲は拡がった。

A2199中心部：磁場の推定

・磁場：単一の強度・スケール、確率1/2で反転するモデル
・電子密度：βモデルを考慮して RMの標準偏差から磁場を計算

$$\sigma_{RM}(r) = \frac{K B n_0 r_c^{\frac{1}{2}} l^{\frac{1}{2}}}{\left(1 + \frac{r^2}{r_c^2}\right)^{\frac{6\beta-1}{4}}} \sqrt{\frac{\Gamma(3\beta - 0.5)}{\Gamma(3\beta)}}$$

(Govoni+.2010)

K	定数(441)
n_0	銀河団のX線中心での電子密度
r_c	コア半径
r	銀河団中心から電波源までの距離
l	ランダム磁場のスケール
β	βモデルのパラメータ

観測値とパラメータの値

σ_{RM}	779.16 $[rad/m^2]$
β	0.663
r_c	$1.16 \times 10^2 h_{70}^{-1}$ [kpc]
n_0	$3.45 \times 10^{-2} [cm^{-3}]$
r	$10 h_{70}^{-1}$ [kpc]
l	5 [kpc]

(Mohr +.1999)

※ 磁場は等方的であると仮定
($\sqrt{3}B_{\parallel} = B$)

$$B \sim 2.27 \left(\frac{l}{5\ kpc}\right)^{\frac{1}{2}} [\mu G]$$

Depolarization because of random magnetic fields

External Faraday Dispersion

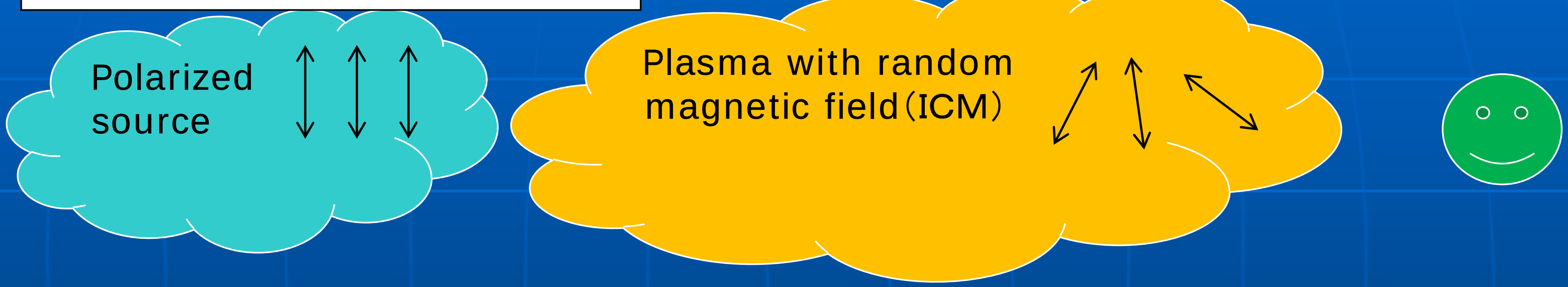

- Because of frequency dependence of FR($\Delta\theta \propto \omega^{-2}$), depolarization is more prominent in lower frequency (or longer wavelength).

$$p_{\mathrm{EFD}} = p_0 e^{-S}$$

$$S = 2\sigma_{\mathrm{RM}}^2 \lambda^4$$

Burn’s law (Burn 1966)
p_{EFD}: observed fractional polarization
p_0: intrinsic fractional polarization
σ_{RM}: standard deviation of RM

Abell 2256

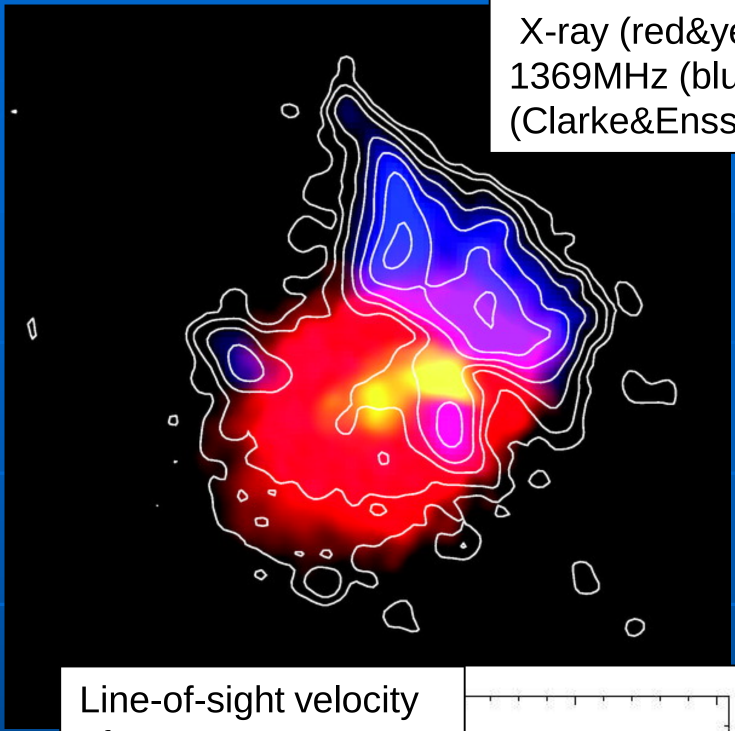

X-ray (red&yellow)
1369MHz (blue&contours)
(Clarke&Ensslin 2006)

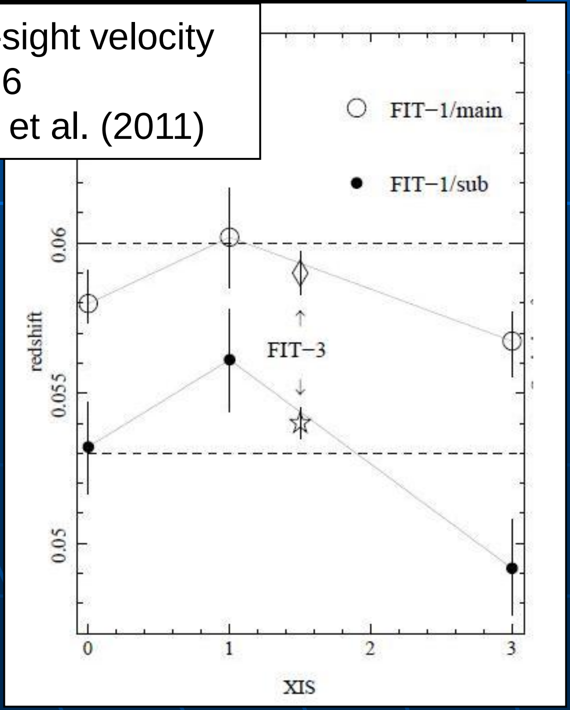

Line-of-sight velocity of A2256
Tamura et al. (2011)

- Well-known local (z=0.0581) merging cluster
- Two components in member galaxy l.o.s. velocity distribution（Berrington et al. 2002）
- Two distinct peaks in X-ray image(Briel et al. 1991, etc)
- Only one example of direct detection of ICM internal motions(～1500km/s) (Tamura et al. 2011)
- Radio halo and relics (Clarke&Ensslin 2006, etc)

Fractioal Polarization Spectra of A2256 Relic (Ozawa et al. 2015)

$$\mathrm{FPOL} = \frac{\sqrt{Q^2 + U^2}}{I}.$$

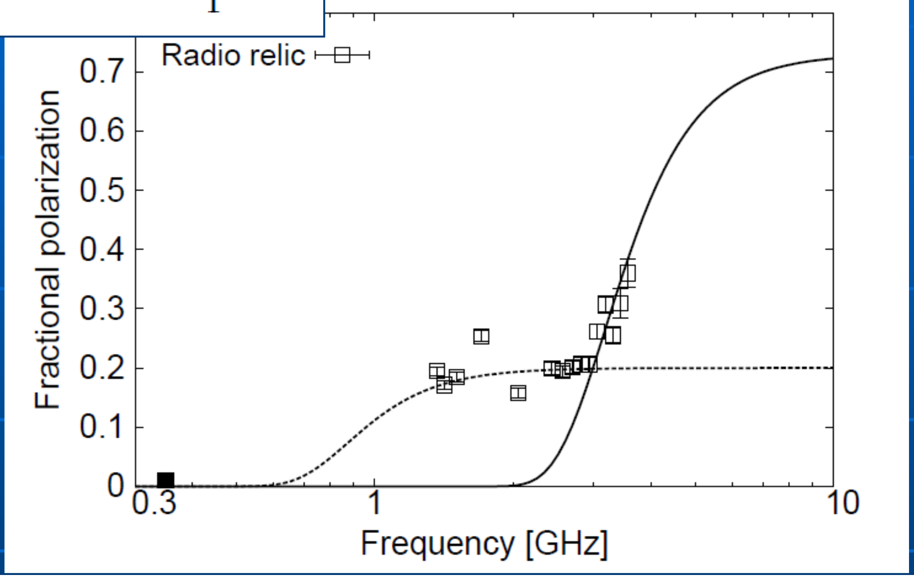

Fractional polarization spectra of the radio relic
FPOL=p exp(-S), (Burn's law)
p: intrinsic FPOL, $S = 2\sigma_{RM}^2 \lambda^4$

- Fractional polarization specta have two distinct strucures（～0.8GHz, ～3GHz）
- Random magnetic field between the relic and us cause depolarization.
- However, a simple external Faraday dispersion (EFD) model cannot reproduce this kind of spectral shape.
- There might be two depolarization components ？？？

simple EFD

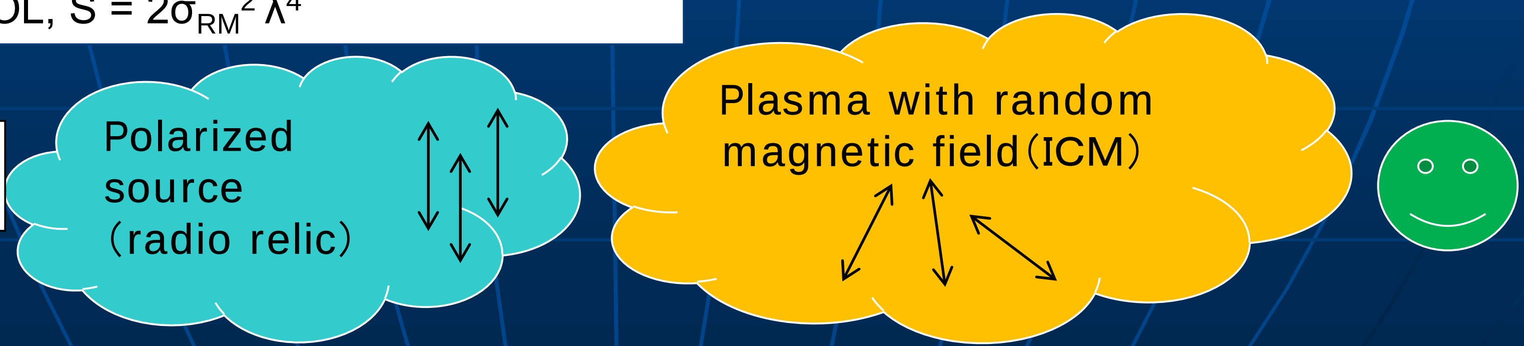

Depolarization toward the A2256 Relic (Ozawa et al. 2015)

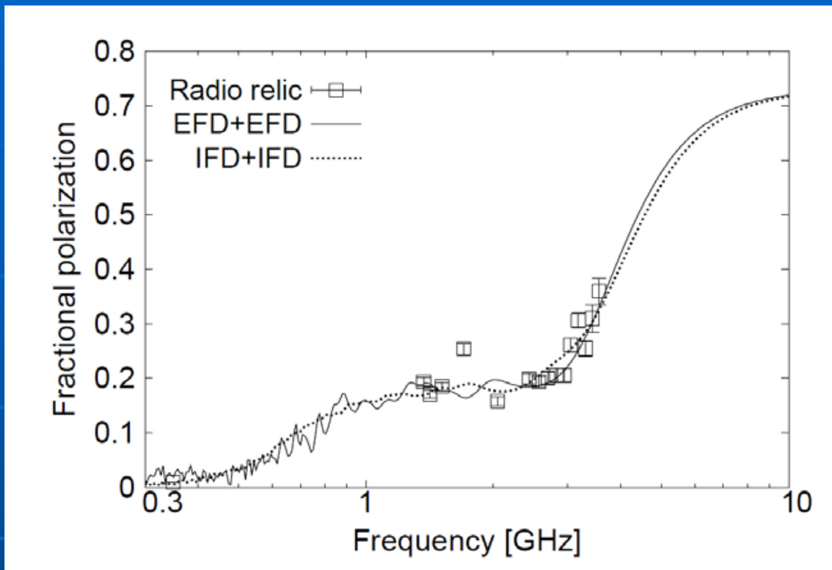

Table 4. Parameters for the Depolarization Models.

Model	Component	B [μG]	n_e [10^{-3} cm^{-3}]	Δl [kpc]	$N_X \times N_Y$ [kpc $\times$ kpc]	N_Z [kpc]	Intensity	$\sigma_{\rm RM}$ [rad m^{-2}]
EFD+EFD	foreside	0.3	3.0	1*	50×50 *	500	1	6.3
	backside	5	10.0			25 †	5	128.5
IFD+IFD	foreside	0.5	1.0	1 *	50×50 *	500	1	5.2
	backside	10	10.0			25 †	4.5	228.3

* We assume 50×50 kpc since the beam size of 47″ corresponds to ~52 kpc.

† We assume that the thickness of the radio relic is 25 kpc (Owen et al. 2014).

EFD+EFD

Polarized sources (relic???)

Depolarization component (relic???)

Polarized source (relic???)

Depolarization component (ICM or Galactic)

IFD+IFD

Polalaized source and Depolarization component (relic???)

Polarized source and Depolarization component (ICM or Galactic)

Summary

- The intracluster magnetic field is investigated with X-ray and Rdaio observations.
  - Radio halos and relics (Itahana's and Takanohashi's talks)
  - Faraday rotation
- The magnetic field plays crucial roles in various process such as particle acceleration in the ICM
- A2199center (Takahashi master thesis)
  - Magnetic field estimation with Faraday rotation
- A2255 (Ozawa et al. 2015)
  - S- and X-band polarimetric observations with JVLA.
  - Fractional polarization spectra of the relic have characteristic structures, which can be reproduced assuming that two depolarization components are located along the line-of-sight.

Rotation Measure

RM map

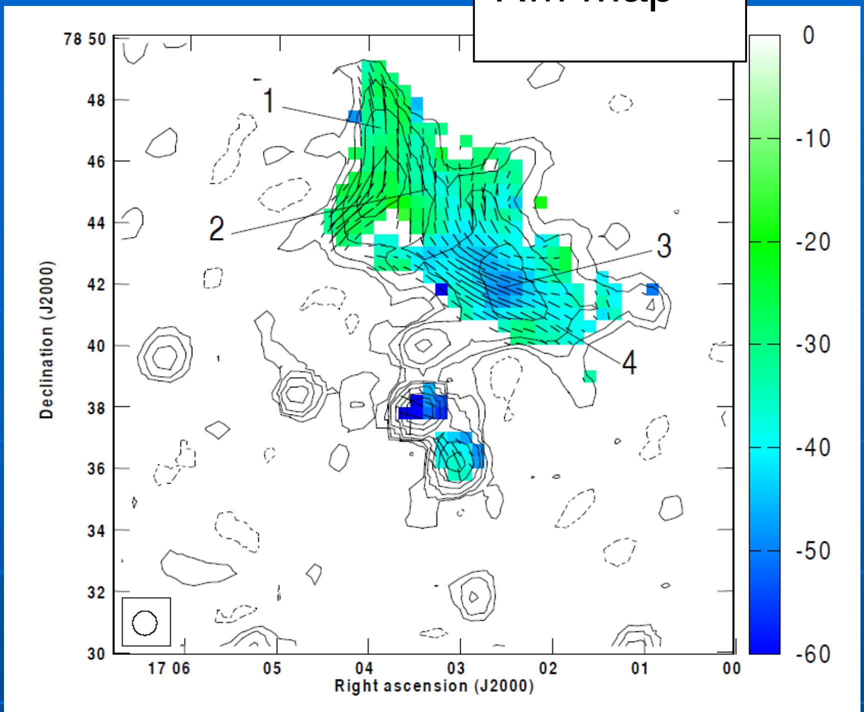

Table 3. The average and standard deviation of RM.

Target	$\langle \mathrm{RM} \rangle^*$ rad m^{-2}	$\sigma_{\mathrm{RM}}{}^*$ rad m^{-2}	reference
Relic	-44	7	Clarke & Ensslin (2006)
Relic	-34.5	6.2	this work
Source A	-24.9	65.5	this work
Source B	-34.1	10.5	this work

* $\langle \mathrm{RM} \rangle$ and σ_{RM} are the average and standard deviation of RM, respectively.

ϕ vs λ^2

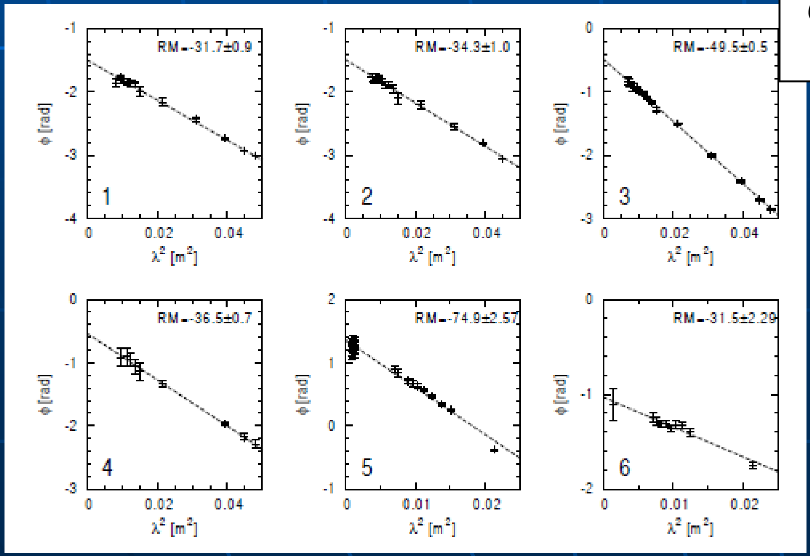

- <RM>～ -30 rad/m^2

  This value is consistent with a contribution from the Galactic component
- In relic, σ_{RM} is significantly smaller than that of sources A.

  -→The relic is located in the nearer side of the observer in the cluster

Observations

Table 1. Details of the VLA & JVLA observations of Abell 2256.

Frequency* (MHz)	Bandwidth* (MHz)	Config.*	Date	Time* (h)	Project*
1369/1417	25/25	D	1999-Apr-28	5.9, 5.9	AC0522
1513/1703	12.5/25	D	1999-Apr-29	3.5, 5.5	
1369/1417	25/25	C	2000-May-29	2.5, 2.5	AC0545
1513/1703	12.5/12.5	C	2000-May-29	3.6, 3.6	
1369/1417	25/25	C	2000-Jun-18	2.5, 2.5	
1513/1703	12.5/25	C	2000-Jun-18	4.1, 3.5	
16 windows†	128	C	2013-Aug-25	1.2	13A-131
S-band			2013-Aug-26	1.2	
			2013-Aug-29	1.2	
16 windows‡	128	C	2013-Aug-18	1.3	13A-131
X-band			2013-Aug-19	1.3	

* Column 1: observing frequency; Column 2: observing bandwidth; Column 3: array configuration; Column 4: dates of observation; Column 5: time on source; Column 6: NRAO project code.

† 2051/2179/2307/2435/2563/2691/2819/2947/3051/3179/3307/3435/3563/3691/3819/3947.

‡ 8051/8179/8307/8435/8563/8691/8819/8947/9051/9179/9307/9435/9563/9691/9819/9947.

- multi-band polarimetric observations, to explore the magnetic field trough depolarization and rotation measure
- S-band (2051-3947MHz)
- X-band (8051-9947MHz)

August 2013, JVLA

- L-band (1369-1703MHz) archive data of VLA

Radio images

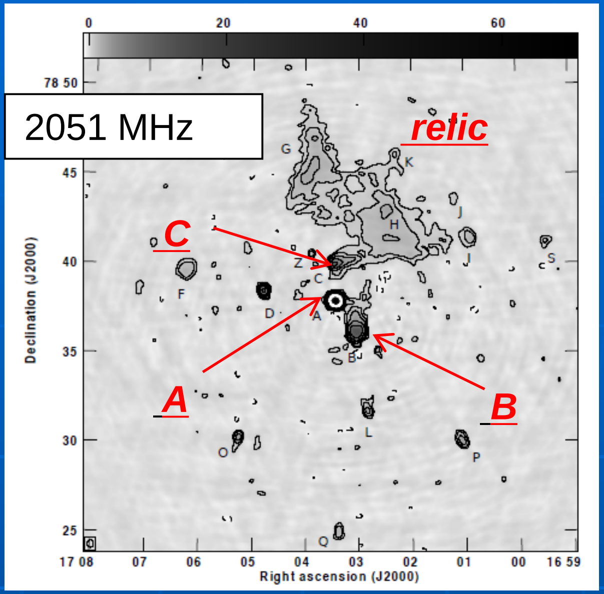

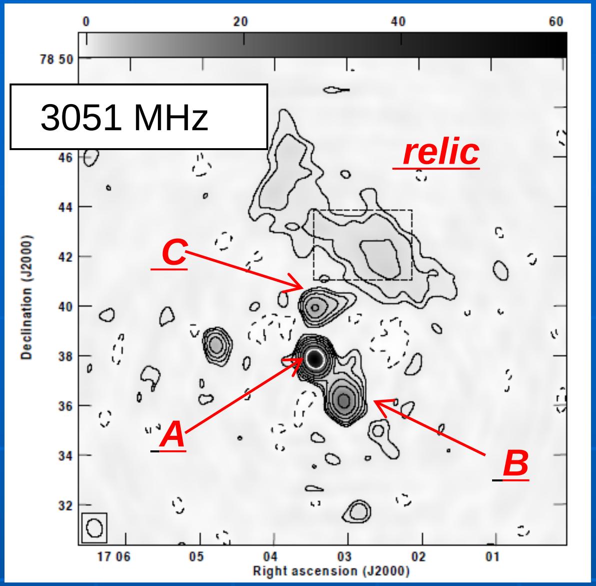

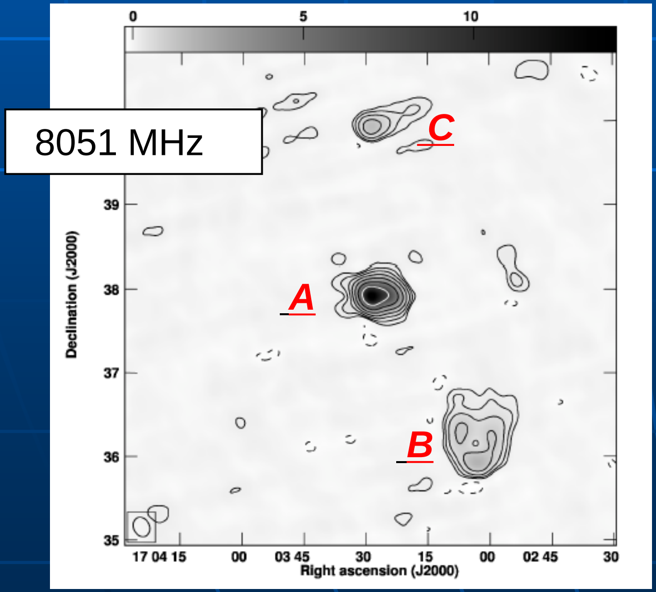

- relic, source A--Z (point sources such as radio galaxies)
- In S-band, polarized components are detected from relic, A, and B
- In X-band, polarized components are detected only from source A（relic is out of FOV）。

Merger geometry and relic formation scenario

Early phase scenario

Late phase scenario

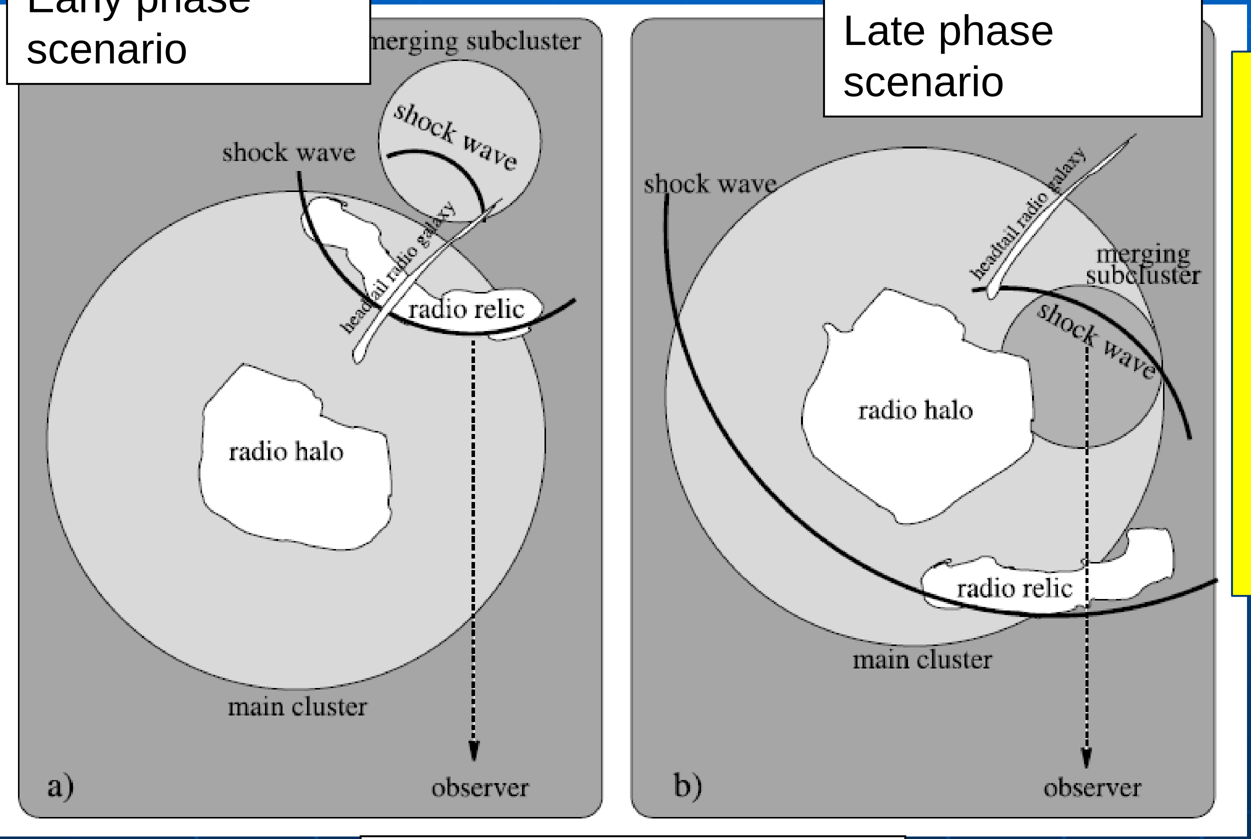

Clarke&Ensslin(2006)

Considering small σ_{RM} value, relic is likely located nearer side of us in the cluster.

This fact favors “Late phase scenario”.

Magnetic Fields toward Source A and B

l: coherent length of the field

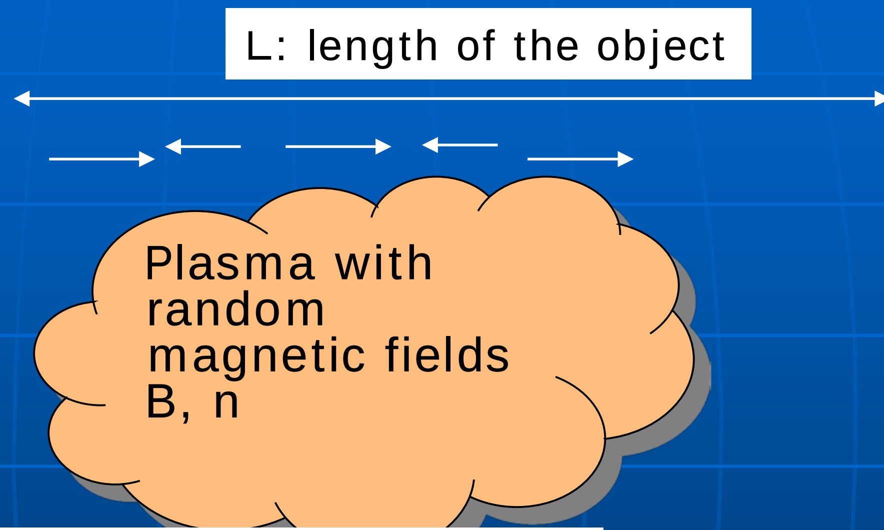

Δθ behaves like random walk processes.
$\Delta\theta \sim \lambda^2 n B_{//} (lL)^{0.5}$

$$\sigma_{\rm RM} = \frac{K B n_0 r_c^{1/2} \Lambda_B^{1/2}}{(1 + r^2/r_c^2)^{(6\beta-1)/4}} \sqrt{\frac{\Gamma(3\beta - 0.5)}{\Gamma(3\beta)}},$$

Table 6. Parameters for magnetic field strengths.

Source	X-ray morphology	K	$\sigma_{\rm RM}$ [rad m^{-2}]	n_0‡ [10^{-3} cm^{-3}]	r** [kpc]	r_c‡ [kpc]	β‡	Λ_B [kpc]	B [μG]
Abell 2256 A	Irregular	441	65.5	2.6	7.2	587	0.914	20–5	0.63–1.26
Abell 2256 B	Irregular	441	10.5	2.6	133.7	587	0.914	20–5	0.11–0.21

Faraday Tomography for the relic

QU-fit for relic

Black lines: two components model

Grey lines: one component model

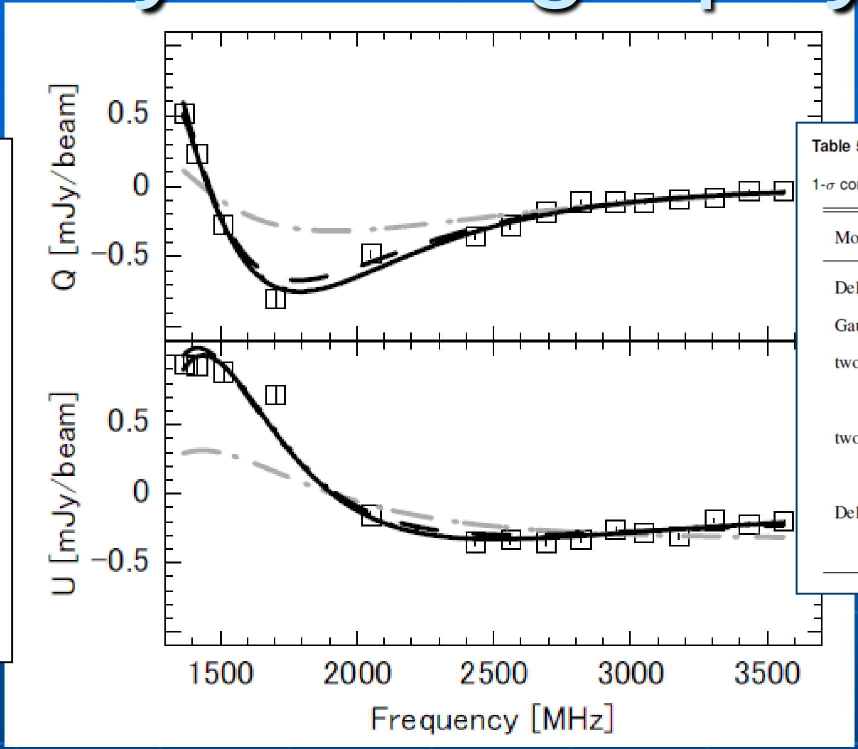

Table 5. The reduced chi-square (RCS), the Bayesian information criterion (BIC), and best-fit values and 1-σ confidence regions for model parameters in the QU-fit.

Model	RCS	BIC	ϕ	Amp.	χ_0	Width
Delta function	38.8	1173.1	$-41.29^{0.713}_{-0.688}$	$0.32^{0.005}_{-0.005}$	$-0.56^{0.009}_{-0.009}$	
Gaussian	38.8	1176.5	$-41.28^{0.704}_{-0.710}$	$0.32^{0.005}_{-0.005}$	$-0.56^{0.009}_{-0.009}$	$0.00^{0.675}_{0.008}$
two Deltas	5.0	170.0	$-46.71^{0.972}_{-0.971}$	$3.86^{0.207}_{-0.049}$	$0.35^{0.051}_{-0.040}$	
			$-43.74^{0.914}_{-1.111}$	$3.92^{0.107}_{-0.054}$	$-1.22^{0.050}_{-0.039}$	
two Gaussians	3.8	142.0	$-40.87^{3.446}_{-0.722}$	$6.14^{0.106}_{-0.231}$	$0.37^{0.009}_{-0.066}$	$11.99^{3.078}_{-0.959}$
			$-38.25^{3.326}_{-0.805}$	$6.20^{0.090}_{-0.242}$	$-1.20^{0.008}_{-0.064}$	$10.43^{1.851}_{-1.034}$
Delta + Ganssian	3.9	139.6	$-57.53^{1.945}_{-0.528}$	$0.70^{0.357}_{-0.233}$	$0.33^{0.020}_{-0.087}$	
			$-34.43^{3.937}_{-7.701}$	$0.74^{0.343}_{-0.236}$	$-1.26^{0.041}_{-0.154}$	$10.01^{6.586}_{-1.297}$

- Farady tolmography（QU-fit、Ideguchi et al. 2014） for the relic
- Two polaried sources at different Faraday depth are necessary.
- Note: In QU-fit, information about polarization angles is also used. However, we can locate polarized sources only in the Faraday depth space (not real space).